ACS APPLIED MATERIALS & INTERFACES

Biological and Medical Applications of Materials and Interfaces

Highly Efficient Target Recycling-based Netlike Y-DNA for Regulation of Electrocatalysis towards Methylene Blue for Sensitive DNA Detection

Yunrui Li, Yuanyuan Chang, Ruo Yuan, and Yaqin Chai

ACS Appl. Mater. Interfaces, **Just Accepted Manuscript** • DOI: 10.1021/acsami.8b08545 • Publication Date (Web): 06 Jul 2018

ACS Publications

is published by the American Chemical Society. 1155 Sixteenth Street N.W., Washington, DC 20036

Highly Efficient Target Recycling-based Netlike Y-DNA for Regulation of Electrocatalysis towards Methylene Blue for Sensitive DNA Detection

Yunrui Li, Yuanyuan Chang, Ruo Yuan*, Yaqin Chai*

Key Laboratory of Luminescent and Real-Time Analytical Chemistry (Southwest University), Ministry of Education, College of Chemistry and Chemical Engineering, Southwest University, Chongqing 400715, PR China

* Corresponding author at: Tel.: +86-23-68252277; Fax: +86-23-68253172.

E-mail address: yuanruo@swu.edu.cn (R.Yuan), yqchai@swu.edu.cn (Y. Q. Chai)

ABSTRACT

In this work, the highly efficient target recycling-based netlike Y-shaped DNA (Y-DNA), which regulated the electrocatalysis of Fe_3O_4@CeO_2-Pt nanoparticles (Fe_3O_4@CeO_2-PtNPs) towards methylene blue (MB) for signal amplification, was developed to prepare a sensitive DNA biosensor for detecting the DNA associated with oral cancer. Specifically, with the help of highly efficient enzyme-assisted target recycling (EATR) amplification strategy, one target DNA input was converted to corresponding plenty of DNA strands S1-Fe_3O_4@CeO_2-Pt and S2-MB output, which could be employed to interact with HP2 immobilized on electrode surface to form stable netlike Y-DNA without any waste of recycling products. Meanwhile, the formation of netlike Y-DNA could regulate electrocatalytic efficiency of Fe_3O_4@CeO_2-PtNPs, inducing the proximity of Fe_3O_4@CeO_2-PtNPs to MB and significantly enhancing electrochemical signal. Further, the signal could also be amplified by Fe_3O_4@CeO_2-PtNPs modified on electrode surface. By virtue of this ingenious design, a novel netlike Y-DNA structure based on highly efficient EATR was simply constructed and successfully applied to an electrochemical DNA biosensor along with electrocatalysis of Fe_3O_4@CeO_2-PtNPs, achieving the sensitive detection of target DNA ranging from 10 fM to 50 nM with a detection limit of 3.5fM. Impressively, the biosensor here demonstrates an admirable method for regulating the electrocatalysis of nanoparticles (NPs) towards substrates to enhance signal, and we believe that this biosensor is a potential candidate for the sensitive detection of target DNA or other disease-related nucleic acids.

KEYWORDS: netlike Y-DNA, Fe_3O_4@CeO_2-PtNPs, electrocatalysis regulation,

highly efficient EATR amplification, electrochemical DNA detection

INTRODUCTION

DNA nanomaterials are considered as a superior biocompatible material for biological research and clinical diagnosis[1] due to their remarkable properties, including high selectivity in molecular recognition,[2] sequence programmability[3] and Watson-Crick model.[4] On biosensor platform, some DNA structures with unique structural features have been applied for accurately quantifying target molecule,[5-8] such as hairpin,[9] G-quadruplexes,[10,11] cruciform,[12] DNA tetrahedron nanostructure,[13-16] Y-shaped DNA (Y-DNA)[17,18] and so on. Among of them, Y-DNA is initially synthesized by Luo′s research group[19,20] and has been extensively used for its uncomplicated structural feature and high stability. For example, many biosensors were successfully built by simply adding two kinds of DNA strands to interact with target DNA for the formation of Y-DNA, achieving fast target DNA detection with low cost.[21-23] Unfortunately, the lack of amplification strategies in these biosensors obviously limits the sensitivity. Recently, some Y-DNA-based electrochemical biosensors combined with diverse recycling amplification strategies are proposed to improve the sensitivity for target detection,[24-28] however, some drawbacks emerge as follows: (1) the implementation of recycling amplification strategies requires additional DNA strands input, increasing the complexity and cost of the system undoubtedly, (2) commonly, multiple DNA strands are released from recycling procedure, while only one kind of them is used to construct Y-DNA and the other output DNA strands do not play any role, thus there is a serious waste problem of recycling products. In addition, the distribution of Y-DNA structures on the electrode

surface is random and irregular in these electrochemical biosensors, limiting the effective immobilization of Y-DNA. Therefore, it is highly meaningful but full of challenges to conquer these difficulties for constructing easier, more efficient and sensitive biosensors.

Nanoparticles (NPs), useful tools, have been widely used for their unique electronic properties, high surface-to-volume ratio and great potential in the immobilization of micromolecule, protein or nucleic acid.[29] Recently, some new properties of metal oxide NPs are dug up, for example, magnetite NPs (Fe_3O_4NPs) not only have been extensively applied in cell isolation, targeted drug delivery, cell imaging and magnetic resonance imaging[30,31] because of their low price, operational stability, promising magnetic properties and magnetic reusability,[32,33] but also have outstanding intrinsic electrocatalytic activity towards the electrochemical reduction of hydrogen peroxide (H_2O_2) and small dye molecules according research foundings,[34-36] fully refreshing the perception that Fe_3O_4NPs are only used for separation.[37,38] However, the electrocatalytic application of Fe_3O_4-containing nanocomposites in biosensors still remains severe defect in biosensors, such as, these Fe_3O_4-containing nanocomposites usually catalyze the substrate existed in solution, resulting in the drawback of large background signal and strong interference.[39,40] In addition, Fe_3O_4-containing nanocomposites are mainly used for immobilizing proteins or nucleic acids on electrode surface, while the distance between Fe_3O_4-containing nanocomposites catalyst and substrates is often overlooked,[41,42] leading to an inevitable problem about distance obstacle, and decreasing the efficiency of catalysis

amplification. Hence, how to remove the distance obstacle is still an urgent task. Inspired by these, we synthesized Fe_3O_4@CeO_2-Pt nanoparticles (Fe_3O_4@CeO_2-PtNPs) and simultaneously made magnetic cores close to the substrate through the assistance of DNA structures, which successfully regulated the electrocatalysis of magnetic cores towards substrate, and conquering the distance obstacle for signal enhancement.

According to the above analysis, aiming at conquering the challenges existed in current Y-DNA-based biosensors as well as significantly improving the electrocatalysis efficiency of Fe_3O_4-containing nanocomposites, highly efficient target recycling-based netlike Y-DNA for regulation of electrocatalysis towards MB was established on biosensor platform for sensitive target DNA detection. The target DNA, called Oral Cancer Overexpressed 1, is associated to oral tumor size and can act as a biomarker for oral cancer. The fabrication of this electrochemical biosensor was illustrated in Scheme 1. Firstly, we synthesized Fe_3O_4@CeO_2-PtNPs, and then HP1 (labeled with MB at the 3′ terminal) was modified on the surface of Fe_3O_4@CeO_2-PtNPs via Pt-S bond. Once target DNA was introduced into this system to hybridize with HP1 to form a double chain, the DNA nicking endonuclease Nt·BstNBI was triggered to cleave HP1 into two pieces (S1-Fe_3O_4@CeO_2-Pt and S2-MB) and then target DNA dissociated from HP1. The liberated target DNA was capable of hybridizing with another un-nicked HP1 and catalyzing next recycling. Therefore, one target DNA input was able to convert multiple HP1 to S1-Fe_3O_4@CeO_2-Pt and S2-MB output, which could be fully utilized to interact with

HP2 immobilized on electrode surface to form netlike Y-DNA, avoiding the waste of recycling products, and realizing highly efficient target recycling. At the same time, the formation of netlike Y-DNA could regulate the proximity of Fe_3O_4@CeO_2-PtNPs to MB, improving the electrocatalysis efficiency for signal enhancement, and achieving sensitive target DNA detection. With such design, this developed electrochemical biosensor not only proposes a highly efficient target recycling amplification strategy for Y-DNA formation, but also paves a promising avenue to regulate the electrocatalysis of NPs towards substrates.

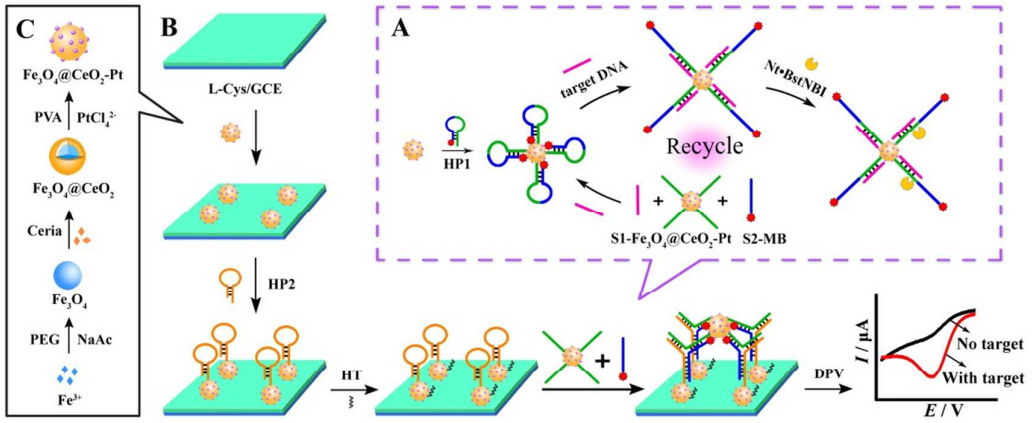

Scheme 1. Scheme of this proposed biosensor for target DNA determination based on highly efficient target recycling to form netlike Y-DNA for regulating the electrocatalysis of Fe_3O_4@CeO_2-PtNPs towards MB: (A) highly efficient EATR amplification, (B) the assembly of the proposed biosensor, (C) the synthesis of Fe_3O_4@CeO_2-PtNPs.

EXPERIMENTAL SECTION

Preparation of Fe_3O_4@CeO_2-Pt Nanoparticles (Fe_3O_4@CeO_2-PtNPs). The Fe_3O_4@CeO_2-PtNPs used in this work were prepared in the light of the published literature study.[43] In the beginning, 3.6 g NaAc, 1.0 g PEG and 1.35 g $FeCl_3 \cdot 6H_2O$

were premixed with EG under ultrasound. And the temperature was adjusted to 200 ºC. Then the Fe_3O_4 precipitate was collected by magnetic separation after 8 h. Secondly, 1 g $Ce(NO_3)_3 \cdot 6H_2O$ was dissolved in 20 mL ethanol containing 1 g NaOH by stirring violently at 50 ºC for 24 h. Then 0.05 mL H_2O_2 (30%) was dropped into the solution. After stirring for 2 h, the precipitate was obtained followed by cleaning and drying. Subsequently, 1 g precipitate was dispersed in 20 mL ultrapure water under continuous ultrasound. The pH was then adjusted to 0.1 and kept at 40 ºC for 2 h to obtain the transparent light-yellow solution. Next, the Fe_3O_4@CeO_2 microspheres were prepared as follows. 3 mL light-yellow solution was mixed with 0.1 g Fe_3O_4NPs and 30 mL ultrapure water. And ammonium hydroxide ($NH_3 \cdot H_2O$) was added to adjust pH to 6.8. After stirring at 60 ºC for 4 h, Fe_3O_4@CeO_2 microspheres were collected by magnetic separation. Finally, 8.0 mL H_2PtCl_6 (1 %) and 0.36 mL of PVA (1 %) were diluted with 60 mL water, followed by the addition of 0.99 mL $NaBH_4$ (0.1 M). When the pH was adjusted to 1.0, 0.1 g Fe_3O_4@CeO_2 microspheres was ultrasonically dispersed in the mixture. After 2 h, Fe_3O_4@CeO_2-PtNPs were obtained by separating and dispersed again for future use.

Preparation of HP1-Fe_3O_4@CeO_2-Pt. Firstly, HP1-Fe_3O_4@CeO_2-Pt bioconjugate was synthesized: 50 μL HP1 (5 μM) was incubated with Fe_3O_4@CeO_2-PtNPs and stirred for 12 h at 4 °C. Next, hexanethiol (HT), one kind of short-chain alkyl molecule, was added to block extra active sites of Fe_3O_4@CeO_2-PtNPs for 40 min. After being rinsed twice, the obtained HP1-Fe_3O_4@CeO_2-Pt was redispersed in 100 μL Tris-HCl.

Highly Efficient Enzyme-assisted Target Recycling Amplification. 30 μL HP1-Fe_3O_4@CeO_2-Pt was mixed with 5 μL Nt·BstNBI (2 U μL^{-1}) and 5 μL target DNA with different concentrations for 1.5 h. During the period, the target DNA hybridized with HP1 to form double-stranded structure, and then the restriction site (5′-GAGTC-3′) which could be specifically recognized by Nt.BstNBI was created. Nt.BstNBI preferentially recognized the site and selectively nicked HP1, resulting that HP1 was cleaved into two pieces (S1-Fe_3O_4@CeO_2-Pt and S2-MB) and target DNA dissociated from HP1. The liberated target DNA was capable of interacting with another HP1 and catalyzed new recycling. By right of this strategy, one target DNA could induce the cleavage of numerous HP1 to obtain plentiful S1-Fe_3O_4@CeO_2-Pt and S2-MB, significantly enhancing the sensitivity for target DNA detection. Finally, the temperature was adjusted to 80 ºC for 20 min to terminate the reaction.

Fabrication of the Proposed Electrochemical Biosensor. The specific process for fabricating the proposed biosensor was performed as follows: Firstly, glassy carbon electrode (GCE) was pretreated by polishing thoroughly with alumina slurries and sonicating for about 5 min. L-Cys, a small amino-containing amino acid, was electrochemically assembled on the cleaned GCE by CV in fresh prepared PBS solution containing 0.02 M L-Cys and 0.1 M HCl with potential ranging from -0.5 to 1.0 V at 100 mV s^{-1} for 15 cycles, which could provide abundant active sites for binding Fe_3O_4@CeO_2-PtNPs through Pt-N bond. After that, Fe_3O_4@CeO_2-PtNPs were immobilized on the surface of L-Cys/GCE electrode at 25 °C, followed by the incubation of 20 μL HP2 (2.5 μM) for 12 h. Next, 10 μL HT (1 mM) was added to

block nonspecific adsorption for 40 min. And the modified electrode was finally incubated with 20 μL the obtained S1-Fe_3O_4@CeO_2-Pt and S2-MB at 37°C for 2 h. After cleaning, the finished electrode could be used for measurements.

Electrochemical Measurements. The EIS and CV electrochemical measurements were carried out in PBS solution (pH 7.4) comprising 5 mM $[Fe(CN)_6]^{4-/3-}$. EIS was measured in the ac frequency ranging from 10^{-1} to 10^5 Hz with an excitation signal of 5 mV and formal potential of 220 mV. CV signal was recorded in potential ranging from -0.2 to 0.6 V at 100 mV s^{-1} scan rate. The DPV response was obtained in PBS solution (0.1 M, pH 7.0) with potential rang of 0.1 V to -0.6 V (vs. SCE), which was used to evaluate the electrochemical performance of the developed biosensor in the most appropriate experimental environment.

RESULTS AND DISCUSSION

Characterization of Fe_3O_4@CeO_2-PtNPs. As Figure 1A and B displayed, the black part in Fe_3O_4@CeO_2-Pt microspheres performed typical TEM image of Fe_3O_4NPs. The bright tiny particles distributed on spheres surface confirmed the successful assemblage of PtNPs, while the rest part of spheres between Fe_3O_4NPs and PtNPs demonstrated the presence of CeO_2. Thus the TEM images fully indicated the successful preparation of Fe_3O_4@CeO_2-PtNPs. Moreover, X-ray photoelectron spectroscopy (XPS) was also utilized to analyze elements for further confirming Fe_3O_4@CeO_2-PtNPs. As shown in Figure 1C, the characteristic peaks for Ce3d, Fe2p, O1s, C1s and Pt4f could be clearly observed in the obtained Fe_3O_4@CeO_2-PtNPs spectrum, which revealed the presence of cerium, iron, oxygen, carbon and platinum

in the sample. The peaks of O1s and C1s could be attributed to the polyvinyl alcohol (PVA) capped on PtNPs. The separate regions of Fe2p and Pt4f were also shown in Figure 1C. The peaks at 711.3 eV and 723.8 eV of Fe2p could be assigned to Fe $2p_{1/2}$ and Fe $2p_{3/2}$, suggesting the existence of Fe_3O_4. And the $Pt4f_{5/2}$ and $Pt4f_{7/2}$ peaks occurred at the binding energy of 71.2 eV and 74.2 eV, indicating that the Pt (0) was stable as metallic state. These results all proved that the Fe_3O_4@CeO_2-PtNPs here were successful synthesized.

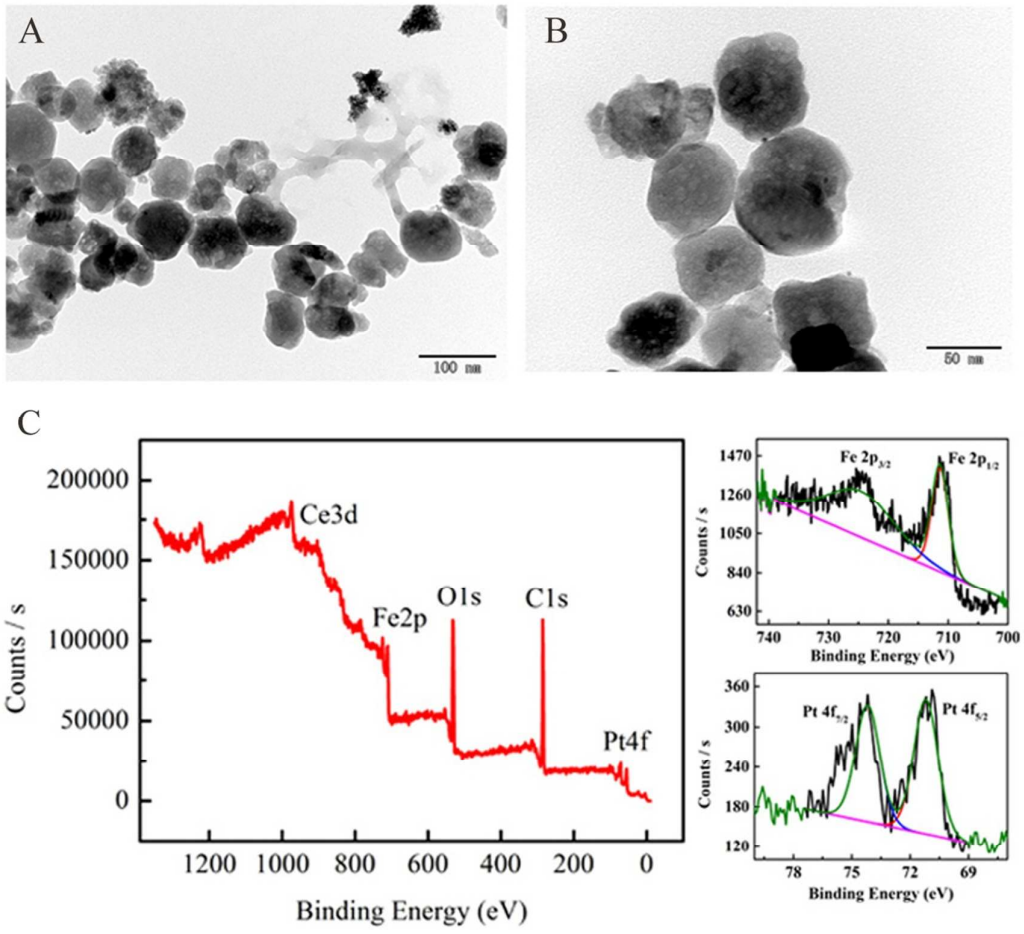

Figure 1. TEM images of Fe_3O_4@CeO_2-PtNPs with (A) 100 nm and (B) 50nm. (C) XPS spectra for the full region of Fe_3O_4@CeO_2-PtNPs, Fe2p region and Pt4f region.

Electrochemical Characterization of the Electrochemical Biosensor. CV and EIS

were utilized to characterize the modification process of the biosensor in 5 mM $[Fe(CN)_6]^{3-/4-}$ solution, respectively. As we can see from Figure 2A and B, the bare GCE (curve a) was electrochemically assembled in the PBS solution containing L-Cys, resulting in decreasing of CV current and increasing of EIS signal (R_{et}) (curve b). Then, Fe_3O_4@CeO_2-PtNPs were introduced onto the surface of L-Cys/GCE to obtain obviously increase of CV and decrease of R_{et} response (curve c) respectively, attributing to the fact that good conductivity of Fe_3O_4@CeO_2-PtNPs could accelerate electron transfer efficiently. When Fe_3O_4@CeO_2-PtNPs/L-Cys/GCE was modified with HP2, a decrease of CV current and an increase of R_{et} response were acquired (curve d) due to the negative charge of HP2. And an obvious decrease of CV current and increase of R_{et} were still be obtained after blocking the electrode surface with HT (curve e), demonstrating that HT greatly blocked electron transfer. All the results showed clearly the successful preparation of the biosensor.

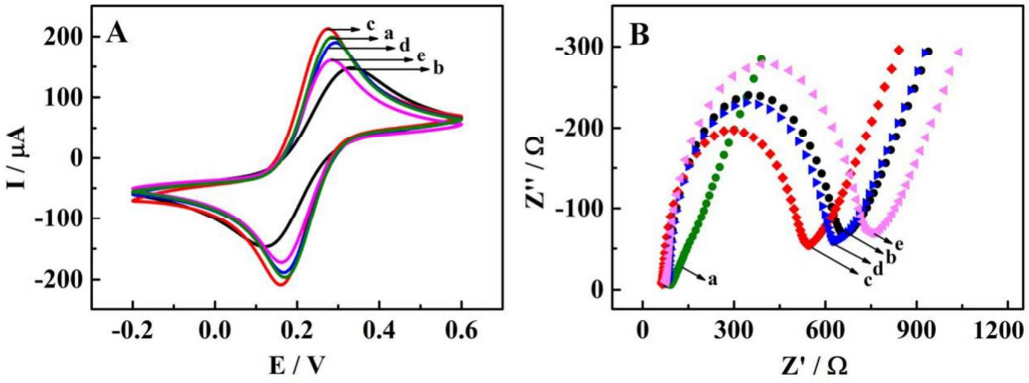

Figure 2. CV (A) and EIS (B) characterizations of the modified electrode at different stages in 5.0 mM $[Fe(CN)_6]^{3-/4-}$ solution: (a) bare GCE, (b) L-Cys/GCE, (c) Fe_3O_4@CeO_2-PtNPs/L-Cys/GCE, (d) HP2/Fe_3O_4@CeO_2-PtNPs/L-Cys/GCE, (e) HT/HP2/Fe_3O_4@CeO_2-PtNPs/L-Cys/GCE.

Optimization of the Reaction Conditions. The nicking reaction of Nt.BstNBI was a

key step for target recycling amplification, thus the effect of Nt.BstNBI nicking reaction time (30 min, 45 min, 60 min, 90 min, 120 min) on the electrode was investigated for 100 pM target DNA. As shown in Figure 3A, with the extension of Nt.BstNBI nicking reaction time, the DPV response increased gradually and reached a plateau after 90 min. Therefore, 90 min was employed as the optimum time of Nt.BstNBI nicking reaction. Furthermore, the incubation time of S1-Fe_3O_4@CeO_2-Pt and S2-MB would affect the formation of netlike Y-DNA, which may cause great influence to the biosensor. Thus, investigating the incubation time of S1-Fe_3O_4@CeO_2-Pt and S2-MB was indispensable. As presented in Figure 3B, the electrochemical signal increased over time and reached its maximum after 120 min. Therefore, 120 min was proved to be the optimum incubation time for preparing biosensor. The error bars presented the standard deviations (SD) of three times parallel tests.

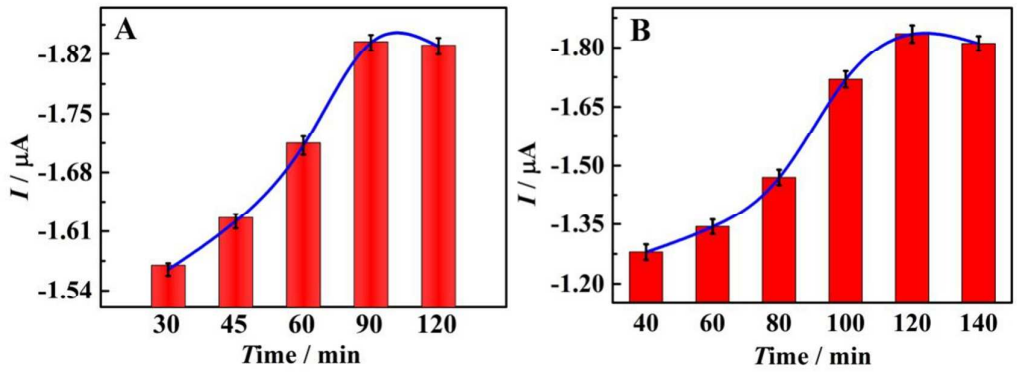

Figure 3. (A) Effect of Nt.BstNBI nicking reaction time on electrode response; (B) optimum incubation time of S1-Fe_3O_4@CeO_2-Pt and S2-MB. The electrochemical signals were obtained with 100 pM target DNA in 0.1 M PBS solution (pH 7.0). Error bars: SD, n = 3.

Comparison of Electrocatalysis Amplification Capability of the Biosensor. To

clarify excellent electrocatalysis of Fe_3O_4@CeO_2-PtNPs, control experiment was conducted to construct two different biosensor platforms B and C. Compared with the proposed biosensor (A) in this work, the only difference of B was that there was no Fe_3O_4@CeO_2-PtNPs involved in target recycling process, while Fe_3O_4@CeO_2-PtNPs were only used as electrode material. C was further to replace electrode material with Au. Under the same and optimal conditions, the DPV responses of the biosensor platforms (A, B, and C) were obtained by using 100 pM target DNA. It was obvious that there was sharp decrease in current responses from A, B to C in Figure 4, which might be ascribed to the following concerns: 1. large surface area exhibited by Fe_3O_4@CeO_2-PtNPs was desired for immobilizing DNA. 2. Fe_3O_4@CeO_2-PtNPs performed more effective signal amplification than Au. 3. Signal amplification was more remarkable when Fe_3O_4@CeO_2-PtNPs were close to MB. In a word, Fe_3O_4@CeO_2-PtNPs in this work had effectively increased the sensitivity of the biosensor.

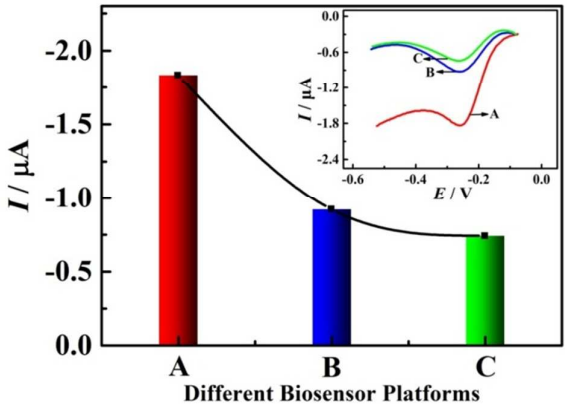

Figure 4. The DPV responses of different biosensor platforms A, B and C.

Analytical Performance of the Proposed Electrochemical Biosensor. Herein, the

analytical performance of the biosensor was demonstrated under optimal reaction conditions by measuring the corresponding DPV responses of different concentrations target DNA in 0.1 M PBS solution (pH 7.0), and all results were displayed in Figure 5A and B. Obviously, the electrochemical signal increased gradually with the increasing concentration of target from 10 fM to 50 nM and possessed a desirable linear relationship with the logarithm of concentration of target DNA. The corresponding linear regression equation was I = -0.1359 log$c$ - 2.007 (r = 0.994), and the limit of detection (LOD) was calculated to be 3.5 fM according to the recommended method of LOD = 3Sb/m (where Sb represents the standard deviation of the blank signals and m is the slope of the calibration curve). Furthermore, this proposed biosensor was compared with previous reports for nucleic acid detection in Table S2. It can be seen from the Table S2, although the proposed biosensor had no prominent advantage in detection time, it is worth noting that it presented outstanding performance with wider response range and lower detection limit, which may be attributed to the highly efficient EATR and Fe_3O_4@CeO_2-PtNPs amplification strategy.

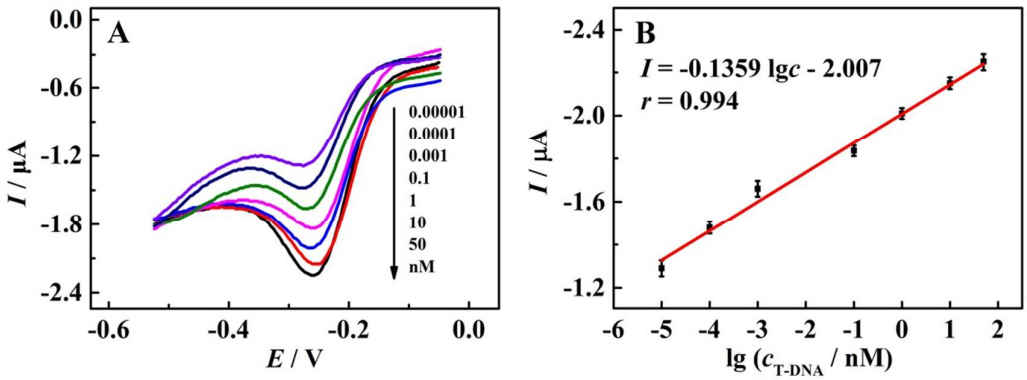

Figure 5. (A) DPV responses of proposed biosensor incubated with various target DNA

concentrations: 0.00001, 0.0001, 0.001, 0.1, 1, 10, and 50 nM in PBS solution (pH 7.0). (B) The calibration plot of peak current versus the logarithm of target DNA concentration. Error bars: SD, n = 3.

Selectivity, Reproducibility and Stability of the Biosensor. In order to assess the selectivity of the proposed electrochemical biosensor, miRNA-21, miRNA-141 and the DNA correlated with Alzheimer's disease (AD-DNA) were chosen as the interference substrates to study the selectivity. As can be seen from Figure 6, the DPV current responses of miRNA-21 (10 nM), miRNA-141 (10 nM) and AD-DNA (10 nM) were almost negligible in comparison with the target DNA (1 nM). Conversely, a high DPV current response could be observed when constructed the biosensor with the mixture (comprising 1 nM target DNA, 10 nM miRNA-21, 10 nM miRNA-141 and 10 nM AD-DNA), and the value is the same as that with only 1 nM target DNA. All above the results demonstrated the excellent selectivity of the biosensors, which was attributed to the extremely specific recognition of Nt·BstNBI. Next, five different batches of the biosensors were prepared under the same conditions to detect 1 nM target DNA respectively for evaluating the reproducibility and precision of the biosensor. As shown in Figure S4, it was found that the electrodes performed similar DPV responses and the batch-to-batch relative standard deviation (RSD) was 5.4%. The results indicated acceptable reproducibility of the biosensor. Moreover, the proposed biosensor was stored at 4 °C and measured every 4 days to monitor the stability. As shown in Figure S4, the electrochemical signal of the biosensor could still maintain 88.4% of the corresponding original response after 20 days, demonstrating

long-term stability of the prepared biosensor.

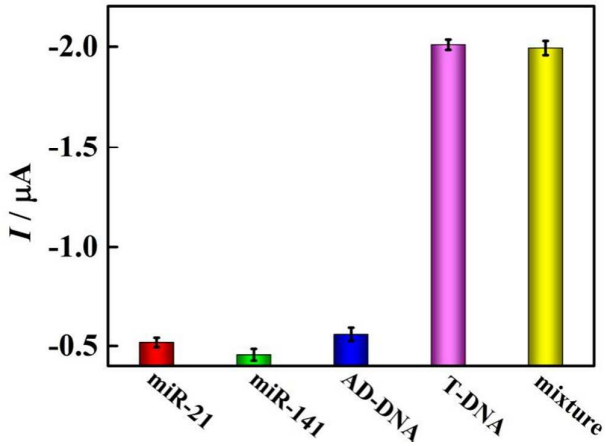

Figure 6. Specificity of the electrochemical biosensor towards target DNA (1 nM) against other nucleic acid: miRNA-21, miRNA-141 and AD-DNA at 10 nM. Error bars: SD, n = 3.

CONCLUSION

In conclusion, we proposed an admirable and economical strategy for the formation of netlike Y-DNA on electrochemical platform to sensitively detect target DNA on the basis of highly effective EATR and Fe_3O_4@CeO_2-PtNPs electrocatalysis amplification. Firstly, stable netlike Y-DNA was constructed by taking the highly effective EATR strategy, realizing full utilization of recycling products. Meanwhile, netlike Y-DNA was also served as a tool to regulate electrocatalysis of Fe_3O_4@CeO_2-PtNPs, resulting in that magnetic cores were close to MB for strong catalysis, significantly enhancing the sensitivity of the biosensor and achieving sensitive target DNA detection. Meaningfully, the biosensor demonstrates a highly effective target recycling amplification strategy for netlike Y-DNA formation, paves a promising path to regulate catalysis of NPs towards substrates, and has admirable universal applicability for the determination of other disaster-related nucleic acids.

ASSOCIATED CONTENT

Supporting Information

Reagents, apparatus, polyacrylamide gel electrophoresis, the X-ray diffraction (XRD) characterization of Fe_3O_4@CeO_2-PtNPs, interference study, the reproducibility and stability of the electrochemical biosensor (Figure S4), the DPV responses of the blank control without target DNA and comparison of this work with other reports for nucleic acid detection (Table S2) were supplied in Supporting Information.

ACKNOWLEDGEMENTS

This paper was financially supported by the National Natural Science Foundation of China (21675129, 21775124, 21575116 and 51473136) and the Fundamental Research Funds for the Central Universities (XDJK2017A001, XDJK2018AA003), China.

REFERENCES

(1) Chao, J.; Zhu, D.; Zhang, Y. N.; Wang, L. H.; Fan, C. H. DNA Nanotechnology-enabled Biosensors. *Biosens. Bioelectron*. **2016**, *76*, 68-79.

(2) Meng, H. M.; Liu, H.; Kuai, H. L.; Peng, R. Z.; Mo, L. T.; Zhang, X. B. Aptamer-integrated DNA Nanostructures for Biosensing, Bioimaging and Cancer Therapy. *Chem. Rev*. **2016**, *45*, 2583-2602.

(3) Seeman, N. C. DNA in a Material World. *Nature* **2003**, *421*, 427-431.

(4) Watson, J. D.; Crick, F. H. C. Molecular Structure of Nucleic Acids. *Nature* **1953**, *171*, 737-738.

(5) Zhu, D.; Song, P.; Shen, J. W.; Su, S.; Chao, J.; Aldalbahi, A.; Zhou, Z.; Song, S.P.; Fan, C.H.; Zuo, X.L.; Tian, Y.; Wang, L.H.; Pei, H. PolyA-Mediated DNA Assembly on Gold

Nanoparticles for Thermodynamically Favorable and Rapid Hybridization Analysis. *Anal. Chem.* **2016,** *88*, 4949-4954.

(6) Chen, L. Z.; Chao, J.; Qu, X. M.; Zhang, H. B.; Zhu, D.; Su, S.; Aldalbahi, A.; Wang, L. H.; Pei, H. Probing Cellular Molecules with PolyA-Based Engineered Aptamer Nanobeacon. *ACS Appl. Mater. Inter.* **2017,** *9*, 8014-8020.

(7) Qu, X. M.; Zhu, D.; Yao, G. B.; Su, S.; Chao, J.; Liu, H. J.; Zuo, X. L.; Wang, L. H.; Shi, J. Y.; Wang, L. H.; Huang, W.; Pei, H.; Fan, C.H. An Exonuclease III-Powered, On-Particle Stochastic DNA Walker. *Angew. Chem. Int. Ed.* **2017,** *56*, 1855 –1858.

(8) Yang, X. F.; Li, J.; Pei, H.; Li, D.; Zhao, Y.; Gao, J. M.; Lu, J. X.; Shi, J. Y.; Fan, C. H.; Huang, Q. Pattern Recognition Analysis of Proteins Using DNA-Decorated Catalytic Gold Nanoparticles. *Small* **2013,** *9*, 2844–2849.

(9) Ling, P. H.; Lei, J. P.; Zhang, L.; Ju, H. X. Porphyrin-Encapsulated Metal-Organic Frameworks as Mimetic Catalysts for Electrochemical DNA Sensing via Allosteric Switch of Hairpin DNA. *Anal. Chem*. **2015**, *87*, 3957-3963.

(10) Hou, T.; Li, W.; Liu, X. J.; Li, F. Label-Free and Enzyme-Free Homogeneous Electrochemical Biosensing Strategy Based on Hybridization Chain Reaction: A Facile, Sensitive, and Highly Specific MicroRNA Assay. *Anal. Chem*. **2015**, *87*, 11368-11374.

(11) Shi, L. J.; Yu, Y. Y.; Chen, Z. G.; Zhang, L.; He, S. J.; Shi, Q. J.; Yang, H. Z. A Label-free Hemin/G-quadruplex DNAzyme Biosensor Developed on Electrochemically Modified Electrodes for Detection of a HBV DNA Segment. *RSC Adv*. **2015**, *5*, 11541-11548.

(12) Matek, C.; Ouldridge, T. E.; Levy, A.; Doye, J. P. K.; Louis, A. A. DNA Cruciform Arms Nucleate Through a Correlated but Asynchronous Cooperative Mechanism. *J. Phys. Chem. B*

2012, *116*, 11616-11625.

(13) Li, N.; Wang, M. M.; Gao, X. N.; Yu, Z. Z.; Pan, W. A DNA Tetrahedron Nanoprobe with Controlled Distance of Dyes for Multiple Detection in Living Cells and in Vivo. *Anal. Chem*. **2017**, *89*, 6670-6677.

(14) Zhou, W. J.; Li, D. X.; Xiong, C. Y.; Yuan, R.; Xiang, Y. Multicolor-Encoded Reconfigurable DNA Nanostructures Enable Multiplexed Sensing of Intracellular MicroRNAs in Living Cells. *ACS Appl. Mater. Inter.* **2016**, *8*, 13303-13308.

(15) Qu, X. M.; Zhang, H. B.; Chen, H.; Aldalbahi, A.; Li, L.; Tian, Y.; Weitz, D. A.; Pei, H. Convection-Driven Pull-Down Assays in Nanoliter Droplets Using Scaffolded Aptamers. *Anal. Chem*. **2017,** *89*, 3468-3473.

(16) Chen, Q. S.; Liu, H. J.; Lee, W.; Sun, Y. Z.; Zhu, D.; Pei, H.; Fan, C. H.; Fan, X. D. Self-assembled DNA Tetrahedral Optofluidic Lasers with Precise and Tunable Gain Control. *Lab Chip* **2013,** *13*, 3351–3354.

(17) Jia, J.; Chen, H. G.; Feng, J.; Lei, J. L.; Luo, H. Q.; Li, N. B. A Regenerative Ratiometric Electrochemical Biosensor for Selective Detecting Hg^{2+} Based on Y-shaped/hairpin DNA Transformation. *Anal. Chim. Acta*. **2016**, *908*, 95-101.

(18) He, H. F.; Dai, J. Y.; Duan, Z. J.; Meng, Y.; Zhou, C. S.; Long, Y. Y.; Zheng, B. Z.; Du, J.; Guo, Y.; Xiao, D. Target-catalyzed Autonomous Assembly of Dendrimer-like DNA Nanostructures for Enzyme-free and Signal Amplified Colorimetric Nucleic Acids Detection. *Biosens. Bioelectron*. **2016**, *86*, 985–989.

(19) Li, Y. G.; Tseng, Y. D.; Kwon, S. Y.; D'Espaux, L.; Bunch, J. S.; Mceuen, P. L.; Luo, D. Controlled Assembly of Dendrimer-like DNA. *Nat. Mater*. **2004**, *3*, 38-42.

(20) Li, Y. G.; Cu, Y. T. H.; Luo, D. Multiplexed Detection of Pathogen DNA with DNA-based Fluorescence Nanobarcodes. *Nat. Biotechnol*. **2005**, *23*, 885-889.

(21) Guo, L. H.; Xu, Y.; Ferhan, A. R.; Chen, G. N.; Kim, D. H. Oriented Gold Nanoparticle Aggregation for Colorimetric Sensors with Surprisingly High Analytical Figures of Merit. *J. Am. Chem. Soc*. **2013**, *135*, 12338-12345.

(22) Li, J. J.; Liu, Q. Y.; Xi, H. Y.; Wei, X. C.; Chen, Z. B. Y-Shaped DNA Duplex Structure-Triggered Gold Nanoparticle Dimers for Ultrasensitive Colorimetric Detection of Nucleic Acid with the Dark-Field Microscope. *Anal. Chem*. **2017**, *89*, 12850-12856.

(23) Li, J.; Qi, X. J.; Du, Y. Y.; Fu, H. E.; Chen, G. N.; Yang, H. H. Efficient Detection of Secondary Structure Folded Nucleic Acids Related to Alzheimer's Disease Based on Junction Probes. *Biosens. Bioelectron*. **2012**, *36*, 142–146.

(24) Xie, H.; Chai, Y. Q.; Yuan, Y. L.; Yuan, R. Highly Effective Molecule Converting Strategy Based on Enzyme-free Dual Recycling Amplification for Ultrasensitive Electrochemical Detection of ATP. *Chem. Commun*. **2017**, *53*, 8368-8371.

(25) Hu, R.; Fu, T.; Zhang, X. B.; Kong, R. M.; Qiu, L. P.; Liu, Y. R.; Liang, X. T.; Tan, W. H.; Shen, G. L.; Yu, R. Q. A Proximity-dependent Surface Hybridization Strategy for Constructing an Efficient Signal-on Electrochemical DNAzyme Sensing System. *Chem. Commun*. **2012**, *48*, 9507-9509.

(26) Bai, L. J.; Chai, Y. Q.; Pu, X. Y.; Yuan, R. A Signal-on Electrochemical Aptasensor for Ultrasensitive Detection of Endotoxin Using Three-way DNA Junction-aided Enzymatic Recycling and Graphene Nanohybrid for Amplification. *Nanoscale* **2014**, *6*, 2902-2908.

(27) Wang, Y. J.; Zhang, X. Y.; Zhao, L.; Bao, T.; Wen, W.; Zhang, X. H.; Wang, S. F. Integrated

Amplified Aptasensor with In-situ Precise Preparation of Copper Nanoclusters for Ultrasensitive Electrochemical Detection of MicroRNA 21. *Biosens. Bioelectron*. **2017**, *98*, 386–391.

(28) Chen, M.; Gan, N.; Li, T. H.; Wang, Y.; Xu, Q.; Chen, Y. J. An Electrochemical Aptasensor for Multiplex Antibiotics Detection Using Y-shaped DNA-based Metal Ions Encoded Probes with NMOF Substrate and CSRP Target-triggered Amplification Strategy. *Anal. Chim. Acta* **2017**, *968*, 30-39.

(29) Kumar, S.; Ahlawat, W.; Kumar, R.; Dilbaghi, N. Graphene, Carbon Nanotubes, Zinc Oxide and Gold as Elite Nanomaterials for Fabrication of Bbiosensors for Healthcare. *Biosens. Bioelectron*. **2015**, *70*, 498-503.

(30) Tartaj, P.; Morales, M. P.; Gonzalez-Carreño, T.; Veintemillas-Verdaguer, S.; Serna, C. J. The Iron Oxides Strike Back: From Biomedical Applications to Energy Storage Devices and Photoelectrochemical Water Splitting. *Adv. Mater*. **2011**, *23*, 5243-5249.

(31) Xuan, S. H.; Wang, F.; Lai, J. M. Y.; Sham, K. W. Y.; Wang, Y. X. J.; Lee, S. F.; Yu, J. C.; Cheng, C. H. K.; Leung, K. C. F. Synthesis of Biocompatible, Mesoporous Fe_3O_4 Nano/Microspheres with Large Surface Area for Magnetic Resonance Imaging and Therapeutic Applications. *ACS Appl. Mater. Inter.* **2011**, *3*, 237-244.

(32) Zang, L. M.; Qiu, J. H.; Wu, X. L.; Zhang, W. J.; Sakai, E.; Wei, Y. Preparation of Magnetic Chitosan Nanoparticles As Support for Cellulase Immobilization. *Ind. Eng. Chem. Res*. **2014**, *53*, 3448-3454.

(33) Venkateswarlu, S.; Lee, D.; Yoon, M. Y. Bioinspired 2D-Carbon Flakes and Fe_3O_4 Nanoparticles Composite for Arsenite Removal. *ACS Appl. Mater. Inter.* **2016**, *8*,

23876-23885.

(34) Zheng, T. T.; Zhang, Q. F.; Feng, S.; Zhu, J. J.; Wang, Q.; Wang, H. Robust Nonenzymatic Hybrid Nanoelectrocatalysts for Signal Amplification toward Ultrasensitive Electrochemical Cytosensing. *J. Am. Chem. Soc*. **2014**, *136*, 2288-2291.

(35) Wu, S. X.; He, Q. Y.; Zhou, C. M.; Qi, X. Y.; Huang, X.; Yin, Z. Y.; Yang, Y. H. Synthesis of Fe_3O_4 and Pt Nanoparticles on Reduced Graphene Oxide and Their Use As a Recyclable Catalyst. *Nanoscale* **2012**, *4*, 2478-2483.

(36) Chen, Z. W.; Yin, J. J.; Zhou, Y. T.; Zhang, Y.; Song, L.; Song, M. J.; Hu, S. L.; Gu, N. Dual Enzyme-like Activities of Iron Oxide Nanoparticles and Their Implication for Diminishing Cytotoxicity. *ACS Nano*. **2012**, *6*, 4001-4012.

(37) Miao, Y. B.; Gan, N.; Ren, H. X.; Li, T. H.; Cao, Y. T.; Hu, F. T.; Yan, Z. D.; Chen, Y. J. A Triple-Amplification Colorimetric Assay for Antibiotics Based on Magnetic Aptamer-enzyme Co-immobilized Platinum Nanoprobes and Exonuclease-assisted Target Recycling. *Analyst* **2015**, *140*, 7663-7671.

(38) Yang, Z. H.; Zhuo, Y.; Yuan, R.; Chai, Y. Q. Highly Effective Protein Converting Strategy for Ultrasensitive Electrochemical Assay of Cystatin C. *Anal. Chem*. **2016**, *88*, 5189-5196.

(39) Wang, L.; Zhang, Y. Y.; Cheng, C. S.; Liu, X. L.; Jiang, H.; Wang, X. M. Highly Sensitive Electrochemical Biosensor for Evaluation of Oxidative Stress Based on the Nanointerface of Graphene Nanocomposites Blended with Gold, Fe_3O_4, and Platinum Nanoparticles. *ACS Appl. Mater. Inter.* **2015**, *7*, 18441-18449.

(40) Li, F. Y.; Jiang, L. P.; Han, J.; Liu, Q.; Dong, Y. H.; Li, Y. Y.; Wei, Q. A Label-free Amperometric Immunosensor for The Detection of Carcinoembryonic Antigen Based on

Novel Magnetic Carbon and Gold Nanocomposites. *RSC Adv*. **2015**, *5*, 19961-19969.

(41) Chen, M.; Hou, C. J.; Huo, D. Q.; Fa, H. B.; Zhao, Y. N.; Shen, C. H. A Sensitive Electrochemical DNA Biosensor Based on Three-dimensional Nitrogen-doped Graphene and Fe_3O_4 Nanoparticles. *Sens. Actuators, B* **2017**, *239*, 421-429.

(42) Miao, P.; Tang, Y. G.; Wang, L. DNA Modified Fe_3O_4@Au Magnetic Nanoparticles as Selective Probes for Simultaneous Detection of Heavy Metal Ions. *ACS Appl. Mater. Inter.* **2017**, *9*, 3940-3947.

(43) Wang, Q.; Li, Y. J.; Liu, B. C.; Dong, Q.; Xu, G. R.; Zhang, L.; Zhang, J. Novel Recyclable Dual-heterostructured Fe_3O_4@CeO_2/M (M = Pt, Pd and Pt-Pd) Catalysts: Synergetic and Redox Eeffects for Superior Catalytic Performance. *J. Mater. Chem. A*. **2015**, *3*, 139-147.

For TOC only

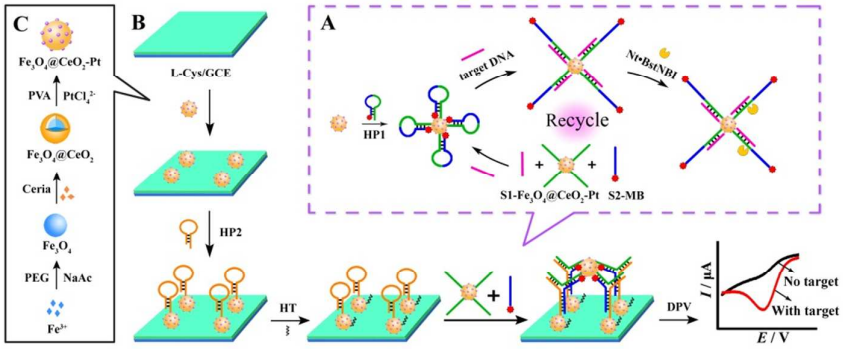
C
Fe_3O_4@CeO_2-Pt
PVA
$PtCl_4^{2-}$
Fe_3O_4@CeO_2
Ceria
Fe_3O_4
PEG
NaAc
Fe^{3+}
B
L-Cys/GCE
HP2
HT
A
target DNA
Nt.BstNBI
HP1
Recycle
S1-Fe_3O_4@CeO_2-Pt
S2-MB
DPV
I / μA
No target
With target
E / V